RESEARCH ARTICLE

Designing an Anatomical Plate to Improve Biomechanics and Stability for Distal Humerus Fractures: FEM Investigation and the Influence of Meshing Strategy

Fahime Rezazade, MSc; Azadeh Ghouchani, PhD

Research performed at University of Isfahan, Isfahan, Iran

Received: 10 April 2026 *Accepted: 28 June 2026*

Abstract

Objectives: Distal humerus fractures require stable fixation to restore elbow function, yet conventional plates often exhibit a geometric mismatch with bone morphology, potentially compromising biomechanical performance. Our finite element analysis (FEA) compared a novel anatomical plate designed to conform to native humeral geometry with a conventional plate for treating type B1 distal humerus fractures. The influence of meshing strategy on the outcomes was also evaluated. Both adaptive and uniform approaches were considered.

Methods: A CT-based three-dimensional humerus model with heterogeneous bone properties was reconstructed from scans of a 37-year-old woman. An anatomically contoured plate was compared with a conventional locking plate. Adaptive and uniform meshing were applied separately to each model, and each construct was subsequently tested under 100 N tensile and compressive loads.

Results: The anatomical plate showed higher stiffness (up to 13%), a broader contact pressure distribution (23–28 MPa vs. conventional: 12–18 MPa), and a larger area of sticking contact, whereas the conventional plate produced higher shear stresses (p=0.113). Uniform meshing generated significantly greater interfragmentary motion than adaptive meshing (p=0.008) but caused unrealistically high screw stresses (up to 1526 MPa). Adaptive meshing predicted higher bone stresses, whereas uniform meshing concentrated stresses in the screws. Although meshing affected the absolute stress and strain magnitudes, the comparative differences between plate designs remained consistent.

Conclusion: The anatomically contoured plate offers greater biomechanical stability than conventional designs for distal humerus fractures, as evidenced by reduced displacement and maintained fragment positioning conducive to healing. An adaptive meshing strategy appears more suitable for FEA of complex fixation components because it yields more reliable stress distributions without altering the primary comparative conclusions. Further experimental validation is warranted before clinical application.

Level of evidence: V

Keywords: Anatomical plate design, Bone plates, Distal, Finite element analysis, Fracture fixation, Humeral fractures, Mesh refinement

Introduction

Distal humerus fractures comprise 2–6% of all fractures and nearly 30% of fractures involving the elbow.[1,2] According to the AO/OTA classification, A1, B1, and C3 fractures are among the most frequently observed subtypes.[3] Managing these fractures poses significant challenges because of the complex osseous anatomy and limited fixation options.[4]

For fractures that cannot be managed using simple noninvasive methods, open reduction and internal fixation (ORIF) is a necessary and reliable surgical technique. Plate geometry and configuration play critical roles in construct stability and successful bone healing.[4] The choice of implant

Corresponding Author: Azadeh Ghouchani, Biomedical Engineering, Department, Faculty of Engineering, University of Isfahan, Isfahan, Iran

Email: a.ghouchani@eng.ui.ac.ir

THE ONLINE VERSION OF THIS ARTICLE
ABJS.MUMS.AC.IR

Copyright © 2026 Mashhad University of Medical Sciences. This work is licensed under a Creative Commons Attribution-Noncommercial 4.0 International License https://creativecommons.org/licenses/by-nc/4.0/deed.en

for type B1 fractures should balance biomechanical stability with minimal surgical invasiveness.

Building on the advantages of anatomically contoured plates for improving fixation stability and reducing soft tissue irritation,[5-8] this study aimed to design an anatomical plate for AO/OTA type B1 distal humerus fractures and biomechanically compare its performance with that of a conventional plate using finite element analysis (FEA).

FEA is a powerful tool for such comparisons, but its reliability is highly dependent on the meshing strategy because mesh density and element type directly influence the accuracy of the results, particularly in geometrically complex regions with high stress gradients.[9] In FEA-based biomechanical studies, uniform and adaptive meshing represent two primary strategies: the former employs a consistent element size throughout the model,[10] whereas the latter adjusts element size according to geometric complexity and stress gradients.[11] Comparing these two meshing approaches under identical conditions helps identify the more suitable strategy for simulating musculoskeletal models with fixation components.

Accordingly, this study had two objectives: first, to compare the biomechanical performance of anatomical and conventional plates for B1 distal humerus fractures; and second, to evaluate the influence of uniform and adaptive meshing strategies on the computational results. These objectives provided a framework for assessing both the relative performance of the plates and the sensitivity of the analysis outcomes to the selected meshing strategy.

Materials and Methods

3D Model Generation

The modeling workflow is summarized in [Figure 1]. Computed tomography scans of a 37-year-old woman without fractures were imported as DICOM files into Mimics (Materialise, Belgium, Research v.21). Subsequently, the cortical and spongy bone regions were segmented separately, and a 3D model of the humerus was generated. A type B1 partial articular fracture of the distal humerus was simulated in 3-Matic (Materialise, Belgium, Research v.13). This fracture involved a portion of the articular surface and extended into the metaphysis while sparing the remaining joint surface. An anatomical plate was contoured to conform to the bone surface. The 3D CAD model of the plate was developed in SolidWorks (Dassault Systèmes, France, v.2022) using a conventional plate profile (a 2.7/3.5 mm locking compression plate , VA-LCP Medial Distal Humerus Plate; DePuy Synthes, Oberdorf, Switzerland)as a dimensional reference.

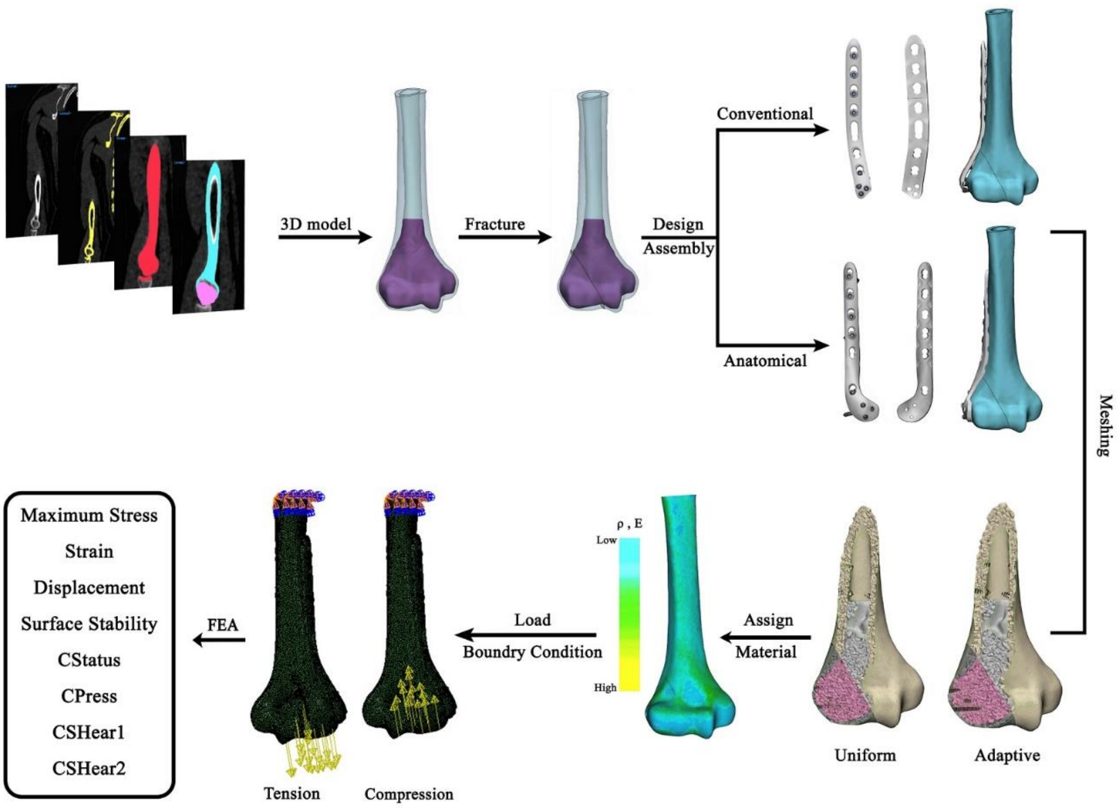

Figure 1. Modeling workflow: A 3D model was generated from CT images, followed by simulation of a type B2 fracture and application of conventional and anatomically contoured plate configurations to the bone model. The final models were meshed using two different mesh types, after which material properties and boundary conditions were defined. The meshed models were subsequently imported into Abaqus for finite element analysis

The thickness of the anatomical plate was specified in 3-Matic. Sharp corners were filleted to prevent stress singularities and reduce computational errors. The contact area between the plate and bone was reduced to preserve the periosteal blood supply.

The anatomical plate retained the same screw-hole pattern (position, number, and size) as the conventional plate. Both models used four 3.5 mm cortical screws and four 3.5 mm locking cancellous screws, ensuring that differences in biomechanical performance were attributable solely to the plate contour. Subsequently, each plate design was separately positioned on the lateral column of the humerus.

Following model assembly, the constructs were meshed with tetrahedral elements using two distinct strategies: adaptive and uniform meshing. The components of these finite element models are labeled in [Figure 2]. The node and element counts and their types for both meshing strategies are summarized in [Table 1]. Bone regions were assigned isotropic material properties, with the elastic modulus varying spatially according to local bone density. The implants were assigned the material properties of stainless steel. The material properties are detailed in [Table 2].[12-14]

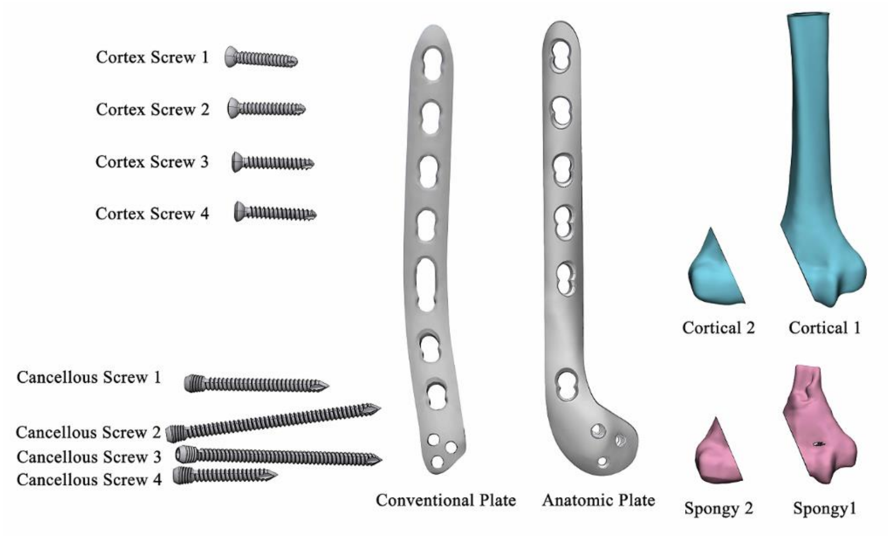

Figure 2. Labeling of the different parts of the models

Table 1. Node and element summary for adaptive and uniform meshing strategies.

Part	Element Number		Node Number	
	Adaptive	*Uniform*	*Adaptive*	*Uniform*
Cortical 1	279,849	244,226	392,747	349,805
Cortical 2	32,504	27,231	51,673	43,044
Spongy 1	130,275	121,856	180,670	167,043
Spongy 2	90,586	79,945	127,472	109,229
Anatomical Plate	84,273	98,043	127,037	144,038
Conventional Plate	65,778	98,824	93,224	144,072
Cortex Screw 1	11,991	8,664	20,833	13,015
Cortex Screw 2	12,085	8,931	21,042	13,461
Cortex Screw 3	12,162	8,614	21,085	12,940
Cortex Screw 4	12,195	8,861	21,063	13,274
Cancellous Screw 1	13,025	29,767	19,011	47,857
Cancellous Screw 2	25,739	55,024	37,286	87,846
Cancellous Screw 3	26,387	54,881	38,210	87,651
Cancellous Screw 4	12,916	29,609	18,851	47,651

Table 2. Material properties of different parts of the models

Part	Elastic modulus (Mpa)	Poisson's Ratio
Cortical bone	E = - 6142 +14ρ (Kg/m3)	0.3
Spongy bone	E= -270 + 4.25ρ (Kg/m3)	0.3
Stainless steel	200000	0.4

Boundary and Loading Conditions

The generated models were imported into Abaqus (Dassault Systèmes, 2022) to apply the boundary and loading conditions. The proximal end of the humerus model was fully constrained, and a 100 N load was applied at the humeroulnar joint [Figure 1] to simulate early postoperative loading.[15] This represented 50% of the clinically acceptable postsurgical load limit of 200 N (approximately 20 kg), reflecting a conservative loading condition.[16]

Tie constraints were defined at the screw–plate interfaces to ensure fully bonded connections, reflecting the rigid fixation typical of locking screw–plate assemblies,[17] and at the cortical–spongy bone interfaces to model bone integrity. Contact within the fracture gap was defined using Abaqus General Contact with a friction coefficient of 0.3.[18]

Analysis Protocol

Four finite element models were analyzed under compression and tension: anatomical and conventional plate constructs, each meshed using uniform and adaptive strategies. Biomechanical metrics, including von Mises stress, strain, displacement, stiffness, contact status, contact pressure, and contact shear stress, were evaluated to compare the mechanical performance of the two plating systems and assess the effects of discretization on the results. Additionally, interfragmentary motion, contact shear stress, and the effects of meshing on stress and strain distributions were statistically evaluated using paired t-tests to determine the significance of the observed differences.

Results

Maximum von Mises Stress

The maximum von Mises stresses in the bone and fixation constructs are reported in [Table 3]. Across loading conditions, cortical bone exhibited comparable stress levels for the two plate designs. In the spongy bone, however, higher stresses were observed with the anatomical plate, whereas the conventional plate produced greater stress concentrations within the fixation construct. Across all analyzed models, the highest stresses within the fixation construct occurred at the screw threads crossing the fracture site.

Regarding the meshing strategy, uniform meshing yielded higher stress magnitudes in the screws, whereas adaptive meshing generally resulted in greater stresses within the bone, except in the cortical region under compressive loading.

Table 3. Maximum Von Mises Stresses in bony parts and the fixation constructs

Maximum von Mises Stress (MPa)	Anatomic Plate				Conventional Plate			
	Adaptive Mesh		Uniform Mesh		Adaptive Mesh		Uniform Mesh	
	Tension	*Compression*	*Tension*	*Compression*	*Tension*	*Compression*	*Tension*	*Compression*
Cortical Bone	101.8	72.3	67.3	81.2	99.7	75.7	72.0	80.1
Spongy Bone	73.5	79.7	54.4	59.9	35.0	37.9	30.3	33.8
Plates	98.7	94.1	44.0	77.7	116.0	55.6	143.4	127.9
Screws	396.6	316.5	725.2	661.6	141.4	74.7	1264.4	1526.6

Strain

Peak strain values were localized within the bone tissue, with spongy bone showing the highest values and the plates the lowest under both tensile and compressive loading conditions [Table 4]. Cortical bone showed similar strain levels with both plate designs, and plate strain remained low, with only minor differences between meshing strategies. In the screws, however, strain in the conventional system was strongly influenced by the meshing method: it decreased with adaptive meshing but increased noticeably with uniform meshing.

With uniform meshing, screw strain in the conventional system was even higher than that in the anatomical plate.

Displacement

Displacement was analyzed for the overall construct and specifically at the fracture gap to evaluate stability [Figure 3]. The conventional plate models generally showed greater overall displacement than the anatomical plate models, except under compressive loading with adaptive meshing. The anatomical plate model exhibited the lowest displacement (0.24 mm) under tension, whereas the conventional plate model showed the highest displacement (0.27 mm); both models had uniform meshing.

Fracture stability under simulated loading was assessed by calculating the net relative displacement across the interface, defined as the difference between the average nodal displacements of the opposing fracture surfaces. This measure represented interfragmentary micromotion. Interfragmentary micromotion was generally higher in the conventional plate models, except under compressive loading with uniform meshing, for which higher values were observed in the anatomical plate model.

A paired t-test was performed on the four adaptive–uniform mesh pairs obtained from both plate types under both loading conditions. Uniform meshing produced significantly greater interfragmentary motion than adaptive meshing ($p = 0.008$).

Table 4. Maximum strain in bony parts and the plate and screw constructs

Maximum Strain (%)	Anatomic Plate				Conventional Plate			
	Adaptive Mesh		Uniform Mesh		Adaptive Mesh		Uniform Mesh	
	Tension	*Compression*	*Tension*	*Compression*	*Tension*	*Compression*	*Tension*	*Compression*
Cortical Bone	1.096	0.767	0.584	0.593	1.072	0.758	0.654	0.522
Spongy Bone	3.767	3.874	6.043	5.400	2.571	1.982	1.614	1.570
Plates	0.048	0.056	0.024	0.035	0.037	0.027	0.036	0.025
Screws	0.26	0.197	0.374	0.366	0.080	0.035	0.586	0.593

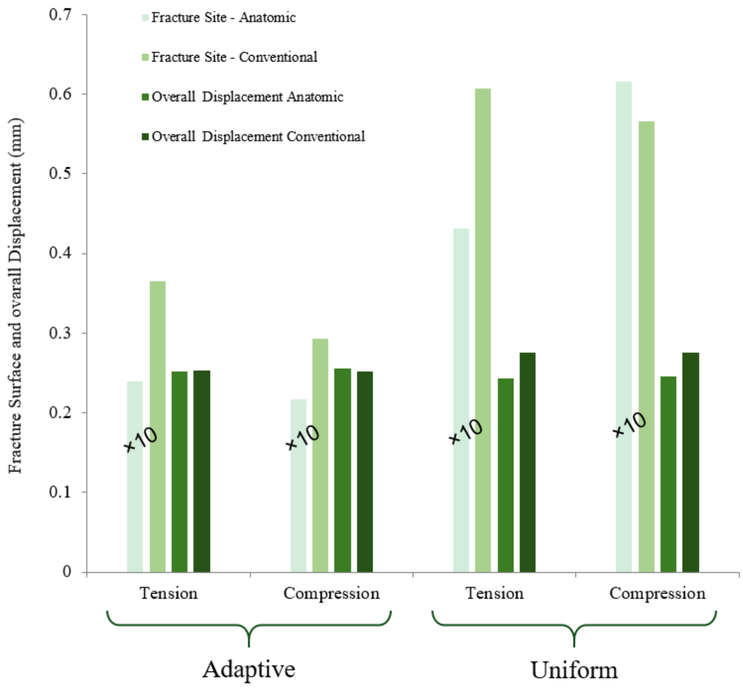

Figure 3. Interfragmentary and overall displacement for the anatomical and conventional plate models. For better visibility, fracture-site displacements are scaled up 10×.

Stiffness

Stiffness was defined as the slope of the force–displacement curve and was calculated by dividing the applied 100-N load by the total displacement of the fixed bone–plate construct. Across all model configurations, anatomical plate fixation generally exhibited greater stiffness than conventional plate fixation under both tensile and compressive loading, with differences of up to 13%. However, under compressive loading with adaptive meshing, the conventional plate exhibited approximately 2% greater stiffness.

Contact Status

The contact status at the fracture site for the two plate models is shown in [Figure 4]. The anatomical plate maintained a larger area of sticking contact, particularly under tension, whereas the conventional plate showed broader regions classified as not in contact. Changing the mesh type from uniform to adaptive resulted in only minor local variations in the overall contact status pattern.

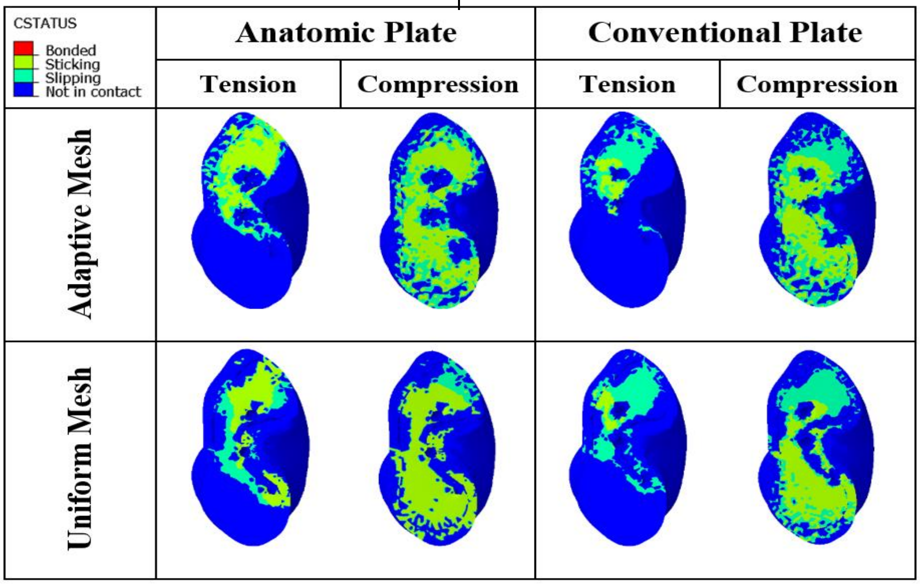

Figure 4. Contact status at the fracture site in the models

Contact Pressure

As shown in [Figure 5], the anatomical plate exhibited a broader and more continuous contact pressure distribution across the fracture interface, indicating more extensive interfacial contact and higher maximum contact pressures (approximately 23–28 MPa). Conversely, the conventional plate showed a more localized and discontinuous pressure distribution, with peak values confined to smaller isolated regions and generally lower maximum pressures (approximately 12–18 MPa). Adaptive meshing generated more refined pressure contours than uniform meshing, whereas the overall distribution patterns and peak pressure locations remained unchanged between the two approaches.

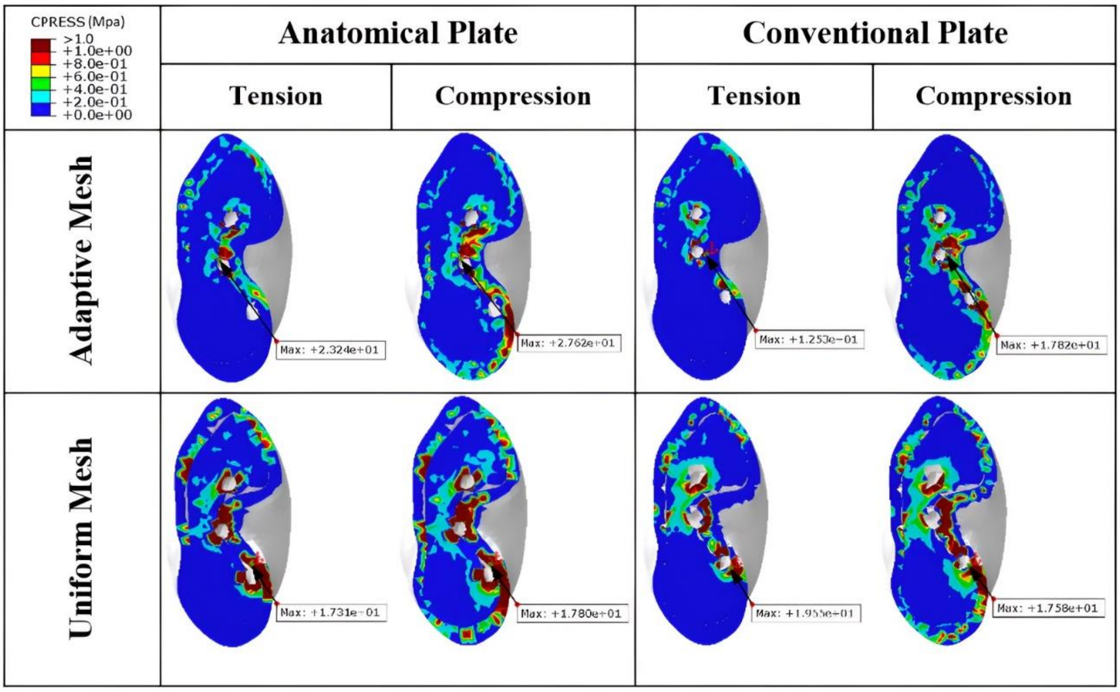

Figure 5. Comparison of contact pressure distribution at the fracture interface across the anatomical and conventional plate models

Contact Shear

Contact shear stresses at the fracture interface were evaluated as the absolute value of the maximum of the two shear components (CSHEAR1 and CSHEAR2). As shown in [Figure 6], the conventional plate consistently exhibited higher peak contact shear stresses than the anatomical plate across all meshing strategies and loading conditions. The magnitude of the difference between the two plates varied with loading and mesh type: it was largest under tensile loading with adaptive meshing and smallest under compressive loading with adaptive meshing. Uniform meshing produced higher maximum contact shear stresses for both plate types than adaptive meshing. Nevertheless, the conventional plate showed greater shear stresses at the fracture interface than the anatomical plate under all conditions. A paired t-test comparing the two plates across the four paired configurations (anatomical vs. conventional under each combination of mesh type and loading condition) indicated that the difference was not statistically significant (P = 0.113).

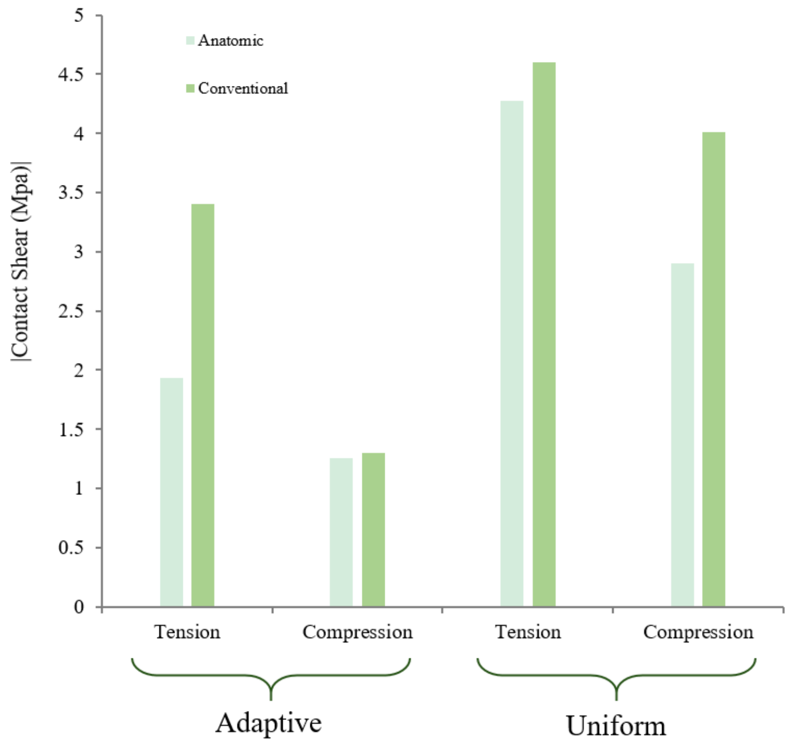

Figure 6. Interfacial shear stress in all models

Role of Meshing

Stress and strain values are shown in [Figure 7A] and [Figure 7B], respectively, with the data plotted against a 45° identity line to assess the influence of mesh type (uniform vs. adaptive) on mechanical outcomes. Points above the line indicate higher values with uniform meshing, whereas points below the line indicate higher values with adaptive meshing. For clarity, simulation scenarios were denoted using a three-letter code indicating the anatomical region (Cor: cortical bone, Spo: spongy bone, Plt: plate, Scr: screws), plate type (Ana: anatomical, Con: conventional), and loading mode (T: tension, C: compression); for example, Cor-Ana-T denotes cortical bone with an anatomical plate under tension.

Adaptive meshing generally predicted higher stresses, particularly in the anatomical plate under tension. In contrast, uniform meshing produced severe stress concentrations in the screws, reaching unrealistically high levels under axial loading. Analysis of strain values showed greater concentrations in spongy and cortical bone under tensile loading with adaptive meshing, whereas the screws in the conventional plate with uniform meshing exhibited markedly higher strain. Despite these pattern differences, paired t-test analysis showed no statistically significant effect of meshing strategy on overall stress (P = 0.094) or strain (P = 0.43).

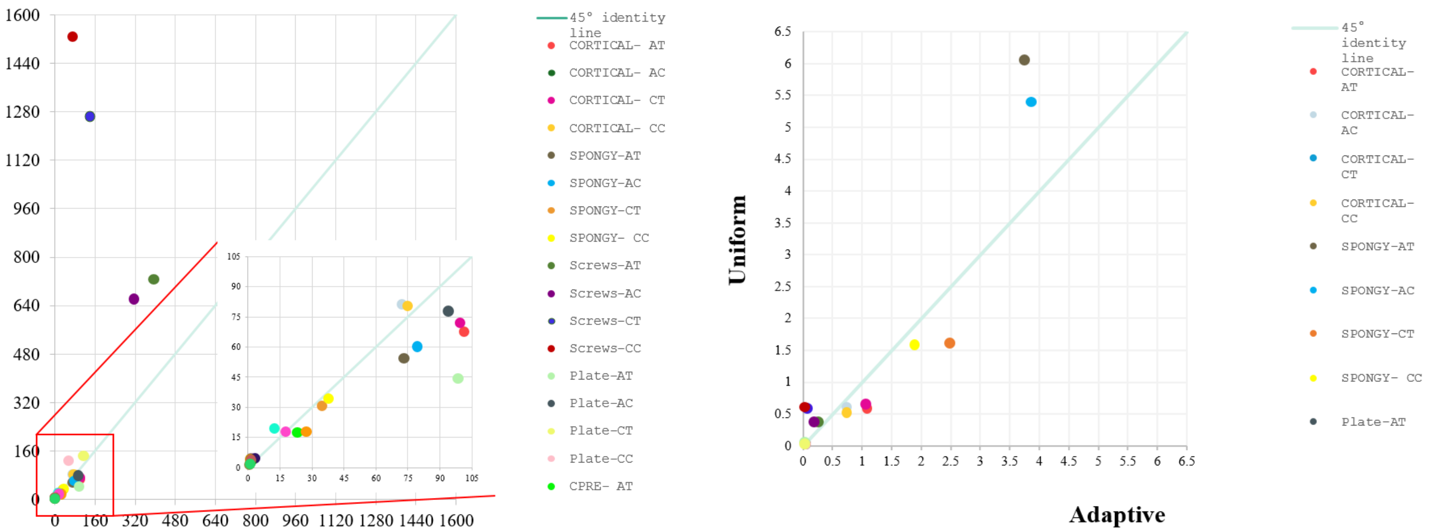

Figure 7. Comparative assessment of the effects of meshing strategies on (A) stress and (B) strain in bony regions and implants

Discussion

Achieving stable anatomical reduction is critical for successful healing after distal humerus fractures. The current gold standard is ORIF with plate fixation; however, conventional plates may exhibit a geometric mismatch with the underlying bone. This incongruence can compromise construct stability and ultimately hinder fracture healing. In contrast, anatomical plates are precontoured to replicate the complex geometry of the distal humerus, thereby offering a theoretical advantage in fixation stability. In this finite element study, an anatomical plate was designed, and its biomechanical performance was compared with that of a conventional plate, with particular emphasis on the influence of adaptive versus uniform meshing on the comparative results.

The present numerical analysis showed that, compared with the conventional plate, the anatomical plate exhibited more stable and balanced mechanical behavior under different loading conditions. The reductions in both overall and interfragmentary displacement in this model were accompanied by improved contact status. With the anatomical plate, contact between the fragments was preserved over a wider area, and fewer regions of separation were observed. This improvement in contact quality was associated with a more uniform distribution of contact pressure, suggesting a more balanced transfer of normal forces across the fracture surface. In addition, the contact shear behavior in the anatomical model showed a more balanced pattern, with lower concentrations of tangential forces that may contribute to fragment slipping or rotation. Overall, the greater contact area and lower contact shear in the model fixed with the anatomical plate, limited fragment displacement and resulted in a stiffer, more stable construct.

Consistent with our findings, Lu et al.[19] demonstrated the superior mechanical stability of anatomical designs for tibial plateau fractures using combined experimental and FEA methods. Their study showed that anatomically contoured fixation reduced fragment displacement compared with conventional constructs. Similarly, Kingsly et al.[20], in a comparative clinical study of displaced midshaft clavicle fractures, showed that precontoured locking plates were associated with greater stability and strength than reconstruction plates.

Stress and strain analyses revealed that the anatomical and conventional models exhibited different load-sharing behaviors. In the conventional model, higher stresses were concentrated within the plate body, with the screws carrying a smaller share of the load. indicating effective load transfer and reduced stress concentrations within the plate. This mechanical response was accompanied by higher strain in the spongy bone, suggesting a more gradual force distribution near the fracture surface. A similar pattern was reported by Hayatbakhsh et al.[21], who found that greater plate conformity in medial opening-wedge high tibial osteotomy increased stress in the locking screw adjacent to the osteotomy site. Consistent with those findings, peak stress in the present study was also concentrated in the screws nearest the fracture site, reinforcing the concept that improved plate conformity shifts load transmission toward the screws and away from the plate body.

A secondary objective of this FEM study was to assess how the meshing strategy influenced the biomechanical response of bone and fixation components. Adaptive meshing is theoretically preferred for complex geometries, such as screw threads and contact interfaces, because it improves local stress resolution, a finding that aligns with our observations.[22] In contrast, uniform meshing produced numerically amplified stresses at these locations, consistent with reports that contact regions and sharp features can generate artificial stress concentrations without adaptive refinement.[23,24] This comparison suggests that adaptive meshing yields more realistic stress and strain distributions within the screws and plate. Nevertheless, parameters such as fracture-fragment contact status were governed primarily by plate design rather than meshing strategy. Overall, although adaptive meshing provides more reliable results for complex fixation components, both mesh types support the study's primary comparative conclusions.

This study has several limitations that suggest directions for future research. First, the finite element model was constructed from CT data from a single healthy woman, which may limit the generalizability of the findings. Future work that includes a broader range of anatomical variations, age groups, and bone qualities would help determine whether the observed trends remain consistent across different populations. Second, the biomechanical environment was simplified by excluding surrounding soft tissues and adjacent joint structures; therefore, the analysis focused primarily on the mechanical behavior of the bone–implant construct. Incorporating these anatomical components into future models may provide a more comprehensive representation of the physiological loading environment. Finally, the loading conditions were limited to axial compression and tension. Future studies that include additional loading modes, such as torsion and bending, could offer a more complete assessment of implant stability under conditions that better reflect daily activities.

Conclusion

This finite element study compared the biomechanical performance of a novel anatomical plate with that of a conventional plate for type B1 distal humerus fractures. The anatomical plate demonstrated superior load transfer to spongy bone and reduced fracture-site displacement, suggesting enhanced construct stability. Although no statistically significant differences were observed between meshing strategies, uniform meshing introduced modeling uncertainties, particularly around screw threads. Collectively, these findings indicate that the anatomical plate offers improved biomechanical performance relative to the conventional design. However, experimental validation remains necessary before clinical translation.

Acknowledgement

N/A

Authors Contribution: Authors who conceived and designed the analysis: Azadeh Ghouchani, Fahime Rezazade/Authors who collected the data: Azadeh Ghouchani/Authors who contributed data or analysis tools: Fahime Rezazade, Azadeh Ghouchani/Authors who performed the analysis: Fahime Rezazade/Authors who wrote the paper: Fahime Rezazade, Azadeh Ghouchani

Declaration of Conflict of Interest: The authors do NOT have any potential conflicts of interest for this manuscript.

Declaration of Funding: The authors received no financial support for the preparation, research, authorship, and publication of this manuscript.

Declaration of Ethical Approval for Study: This study was a computational finite element analysis and did not involve human participants, identifiable patient data, human tissue samples, or animal experiments. Therefore, ethical approval was not required.

Declaration of Informed Consent: This manuscript does not contain any identifiable patient information, including names, initials, hospital identification numbers, clinical images, or photographs. Therefore, informed consent was not required.

Fahime Rezazade MSc [1]
Azadeh Ghouchani PhD [1]

1 Department of Biomedical Engineering, Faculty of Engineering, University of Isfahan, Isfahan, Iran

References

1. Ring D, Jupiter JB. Fractures of the distal humerus. Orthop Clin North Am. 2000;31(1):103-113. doi:10.1016/s0030-5898(05)70131-0.
2. Rose SH, MELTON III LJ, Morrey BF, Ilstrup DM, Riggs BL. Epidemiologic features of humeral fractures. Clin Orthop Relat Res. 1982;168:24-30.
3. Kong G, Mustafa A, Ajaj A, et al. Distal humerus fractures: epidemiology and surgical management trends in hospitalized patients in Qatar. JSES Int. 2025;9(3):902-906. doi: 10.1016/j.jseint.2025.01.005.
4. Savvidou OD, Zampeli F, Koutsouradis P, et al. Complications of open reduction and internal fixation of distal humerus fractures. EFORT Open Rev. 2018;3(10):558-567. doi:10.1302/2058-5241.3.180009.
5. Yetter TR, Weatherby PJ, Somerson JS. Complications of articular distal humeral fracture fixation: a systematic review and meta-analysis. J Shoulder Elbow Surg. 2021;30(8):1957-1967. doi:10.1016/j.jse.2021.02.017.
6. Ahmad M, Nanda R, Bajwa AS, Candal-Couto J, Green S, Hui AC. Biomechanical testing of the locking compression plate: when does the distance between bone and implant significantly reduce construct stability? Injury. 2007;38(3):358-364. doi:10.1016/j.injury.2006.08.058.
7. Schmutz B, Rathnayaka K, Albrecht T. Anatomical fitting of a plate shape directly derived from a 3D statistical bone model of the tibia. J Clin Orthop Trauma. 2019;10:S236-S241. doi: 10.1016/j.jcot.2019.04.019.
8. Shang Y, Bi Y, Cao Y, Wang Y. Finite element analysis of titanium anatomic plate and titanium reconstructive plate for treatment of extra-articular fractures of the scapula. J Orthop

Surg Res. 2023;18(1):134. doi: 10.1186/s13018-023-03614-x.

9. Madier D. An introduction to the fundamentals of mesh generation in finite element analysis. FEA Academy. 2023.
10. Chernikov AN, Chrisochoides NP. Parallel guaranteed quality Delaunay uniform mesh refinement. SIAM Journal on Scientific Computing. 2006;28(5):1907-1926. doi:10.1137/050625886.
11. Hinton E, Rao N, Özakça M. Mesh generation with adaptive finite element analysis. Advances in engineering software and workstations. 1991;13(5-6):238-262. doi:10.1016/0961-3552(91)90030-8.
12. Schneider R, Faust G, Hindenlang U, Helwig P. Inhomogeneous, orthotropic material model for the cortical structure of long bones modelled on the basis of clinical CT or density data. Computer methods in applied mechanics and engineering. 2009;198(27-29):2167-2174. doi:10.1016/j.cma.2009.02.010.
13. Rho J-Y, Hobatho M, Ashman R. Relations of mechanical properties to density and CT numbers in human bone. Med Eng Phys. 1995;17(5):347-355. doi:10.1016/1350-4533(95)97314-f.
14. Wee H, Reid JS, Chinchilli VM, Lewis GS. Finite element-derived surrogate models of locked plate fracture fixation biomechanics. Ann Biomed Eng. 2017;45(3):668-680. doi: 10.1007/s10439-016-1714-3.
15. Goel V, Singh D, Bijlani V. Contact areas in human elbow joints. J Biomech Eng. 1982;104(3):169-75. doi: 10.1115/1.3138344.
16. Verstuyft L, Caekebeke P, van Riet R. Postoperative rehabilitation in elbow surgery. J Clin Orthop Trauma. 2021;20:101479. doi:10.1016/j.jcot.2021.101479.
17. MacLeod AR, Pankaj P, Simpson AHR. Does screw–bone interface modelling matter in finite element analyses? J Biomech. 2012;45(9):1712-1716. doi:10.1016/j.jbiomech.2012.04.008.
18. Shockey J, Von Fraunhofer J, Seligson D. A measurement of the coefficient of static friction of human long bones. Surface Technology. 1985;25(2):167-173. doi:10.1016/0376-4583(85)90030-5.
19. Lu Y, Bai H, Wang Q, et al. The study of biomechanics and finite element analysis on a novel plate for tibial plateau fractures via anterolateral supra-fibular-head approach. Sci Rep. 2023;13(1):13516. doi: 10.1038/s41598-023-47575-x.
20. Kingsly P, Sathish M, Ismail NDM. Comparative analysis of functional outcome of anatomical precontoured locking plate versus reconstruction plate in the management of displaced midshaft clavicular fractures. J Orthop Surg (Hong Kong). 2019;27(1):2309499018820351. doi:10.1177/2309499018820351.
21. Hayatbakhsh Z, Farahmand F, Karimpour M. Is a complete anatomical fit of the Tomofix plate biomechanically favorable? A parametric study using the finite element method. Arch Bone Jt Surg. 2022;10(8):712. doi:10.22038/ABJS.2022.60928.3003.
22. Roarty CM, Grosland NM. Adaptive meshing technique applied to an orthopaedic finite element contact problem. Iowa Orthop J. 2004;24:21.
23. Comninou M. Stress singularity at a sharp edge in contact problems with friction. Zeitschrift für angewandte Mathematik und Physik ZAMP. 1976;27(4):493-499. doi:10.1007/BF01594906.
24. Zienkiewicz OC, Zhu JZ. A simple error estimator and adaptive procedure for practical engineerng analysis. International journal for numerical methods in engineering. 1987;24(2):337-357. doi:10.1002/nme.1620240206.